Excitons in Si nanocrystals: Confinement and migration effects

Johannes Heitmann,* Frank Müller, Lixin Yi, and Margit Zacharias†
Max-Planck-Institut für Mikrostrukturphysik, Weinberg 2, 06120 Halle, Germany

Dmitri Kovalev
Technische Universität München, Physik, Department E16, 85747 Garching, Germany

Frank Eichhorn
Forschungszentrum Rossendorf, Institut für Ionenstrahlphysik und Materialforschung, P.O. Box 510119, 01314 Dresden, Germany
(Received 27 January 2004; published 21 May 2004)

A detailed analysis of the strong room-temperature photoluminescence (PL) signal of size controlled nc-Si is reported. The size control of nc-Si is realized by evaporation of SiO/SiO_2 superlattices and subsequent thermally induced phase separation. By this method the synthesis of completely SiO_2 passivated Si nanocrystals with a controlled size is demonstrated. A strong blueshift of the photoluminescence signal from 1.3 to 1.65 eV with decreasing crystal size is observed. Resonant photoluminescence measurements prove the breakdown of the *k*-conservation rule for nc-Si by showing an increase in the no-phonon transition probability with decreasing crystal size. A no-phonon to phonon assisted transition probability ratio above 1 is detected at 4.5 K. These results confirm quantum confinement as the origin of the investigated luminescence signal. The size dependence of the different luminescence properties and the very high no-phonon transition probability indicate a lower confinement barrier compared to other systems containing nc-Si and additional migration effects of the excitons between the nanocrystals. A separation of quantum confinement and migration effects on the PL signal is possible due to the very narrow size distribution of the nc-Si and detailed time and temperature dependent investigations of the photoluminescence.

DOI: 10.1103/PhysRevB.69.195309 PACS number(s): 78.67.Bf, 78.55.−m, 81.07.Ta

I. INTRODUCTION

After initial reports on room temperature light emission of porous Si[1,2] in the red and near infrared (NIR) region of the spectrum, interest in the optical properties of Si nanocrystals (nc-Si) has grown over the last decade.[3–5] Their compatibility with common microelectronic device fabrication materials and techniques make them attractive for potential applications in integrated optoelectronic devices. A debate as to whether this luminescence band is caused by quantum confinement,[6] defects at the nanocluster surface,[7] by excitation via the nanocluster–nanocluster interface,[7] by Si–Si bonds within the nanocluster itself,[8] or by oxide-related defect states[9] is still on-going. The influence of the wide variation in the synthesis processes might be one reason for the different explanations of the origin for the red luminescence from nc-Si systems. For porous Si the excitonic character of the observed PL signal was clearly shown and quantum confinement effects on the confined excitons were analyzed.[10,11] The results are in good quantitative agreement with the quantum confinement model. For nc-Si embedded in an SiO_2 matrix the results of the optical characterization differ quantitatively from theory which frequently results in different explanations of the observed photoluminescence (PL) signal as described above.

Different processes for the nc-Si synthesis in SiO_2-like Si ion implantation into high quality oxides,[7] sputtering of Si rich oxides,[12] or reactive evaporation of Si rich oxides[13] were in use. One problem for quantitative analysis of the PL signal of nc-Si is the broad and uncontrolled size distribution. Therefore quantum confinement effects and their size dependence are difficult to decouple from possible exciton migration effects. For size-selective PL measurements often the number of excited nanocrystals having a certain size is too low. Within the above-described synthesis methods the Si crystal size is controlled by the Si content in the SiO_2 matrix. Therefore nanocrystal sizes and their concentrations cannot be controlled independently. Last years significant effort was devoted to the independent control of these properties by using the low-energy cluster beam deposition technique (LECBD),[14] co-pyrolysis of disilane,[15] by the preparation of single Si dot multilayers by low-pressure chemical vapor deposition (LPCVD),[16] and finally by the phase separation of SiO/SiO_2 superlattices.[17] Especially the last method allows the synthesis of a dense array of quasimonodisperse Si nanocrystals which are an ideal candidate for a detailed characterization of quantum confinement and migration effects of excitons in the nc-Si as will be shown in this work.

II. CONFINEMENT EFFECTS IN nc-Si: MODEL AND NOTATIONS

Light emission from photoexcited Si is a rather inefficient process due to the indirect nature of the Si band gap. For a recombination of electrons from the minimum of the conduction band ($\Delta_{1,C}$) with holes from the maximum of the valence band ($\Gamma_{25'}$) the contribution of momentum conserving TO or TA phonons is necessary. The spatial confinement of electron and hole within the Si quantum dot results in a smearing out of the electron and hole wave function in *k* space, due to the Heisenberg uncertainty relation. This results in an increasing probability of quasidirect transitions

with decreasing dot size as has been experimentally confirmed for porous Si.[18] Additionally, an increasing energy difference between electron and hole with decreasing crystal size occurs. On the other hand, the exciton binding energy increases with decreasing crystal size which has been estimated to be $-3.572e^2/(\varepsilon_0 d)$, where d is the diameter of the nanocrystal.[19,20] In the following we will always refer the net blueshift of the energy difference between the confined electron and hole as confinement energy E_C in accordance with other theoretical and experimental work.[10,11,18,19,21] This net increase of E_C scales with $D^{-1.3}$ according to theoretical calculations[19,22] under the assumption of infinite confinement potentials. This was proven before experimentally for porous Si (Ref. 18) as well as for nc-Si produced by LECBD.[21] Assuming a finite potential barrier as in the case of nc-Si embedded in a SiO_2 matrix, and taking the abrupt change of the effective mass between nc-Si and the SiO_2 matrix into account a decrease of the power dependence of E_C up to $D^{-1.0}$ is predicted by theory.[23]

An additional contribution to the confinement energy is caused by the electron–hole exchange interaction. It results in a splitting of the exciton energy level into triplet and singlet states assuming that the spin–orbit interaction is rather weak.[10] The quantum-confined-enhanced splitting energy is $\Delta E_X = \Delta E_X^{\mathrm{Si}}(d_X/d)^3$, where $\Delta E_X^{\mathrm{Si}} = 3.165\times 10^{-4}$ eV and $d_X = 4.3$ nm.[24] ΔE_X values between 5 and 20 meV were measured for Si nanocrystals.[10,11,25,26] The radiative lifetime of the electron–hole recombination represents the thermal equilibrium of the lifetime of triplet and singlet state as described by Calcott *et al.*:[10]

$$\tau_r(E,T) = \tau_{\mathrm{trip}}\left(\frac{1+\frac{1}{3}\exp\left(-\frac{\Delta E_X}{k_B T}\right)}{1+\frac{\tau_{\mathrm{trip}}}{3\tau_{\mathrm{sing}}}\exp\left(-\frac{\Delta E_X}{k_B T}\right)}\right), \qquad (1)$$

with τ_{sing} and τ_{trip} as radiative lifetime of singlet and triplet state, respectively. The triplet transition lifetime becomes finite due to the spin–orbit interaction and the geometry of the confinement potential[27] with values between 1 and 15 ms reported so far. For the singlet lifetime values between 1 and 15 μs were measured, depending on the emission energy of the nc-Si.[10,11,25,26]

Additionally, a migration of the excitons between neighboring nanocrystals in porous silicon has been shown to influence its optical properties. An exciton has not only the possibility to recombine radiative or nonradiative but also to migrate to another nanocrystal. This process is favored for silicon nanocrystals by extremely long radiative lifetimes of excitons in the entire temperature range.

Therefore the rate equation of excitons within a Si nanocrystal changes to:[24]

$$\frac{dN_i(t)}{dt} = -\frac{N_i}{\tau_r} - \frac{N_i}{\tau_{\mathrm{nr}}} - \sum_j P_{ij}N_i(t) + \sum_j P_{ji}N_i(t), \qquad (2)$$

where $N_i(t)$ is the number of excitons in the nanocrystal i and P_{ij} the probability for an exciton to migrate from the nanocrystal i to the nanocrystal j. This probability depends on the energy difference between excitons in the nanocrystals i and j (ΔE_{ij}) and their distance (r_{ij}):[24]

$$P_{ij} = \upsilon\cdot\exp(-\gamma\cdot r_{ij}) \quad \text{for } \Delta E_{ij} \leqslant 0, \qquad (3)$$

$$P_{ij} = \upsilon\cdot\exp(-\gamma\cdot r_{ij})\cdot\exp\left(-\frac{\Delta E_{ij}}{k_B T}\right) \quad \text{for } \Delta E_{ij} \geqslant 0. \qquad (4)$$

υ stands for the attempt frequency of the hopping of the exciton. The potential barrier due to the surrounding SiO_2 matrix is implied in the γ factor. This mechanism is called ''trapped controlled hopping mechanism'' [24] and is based on exciton migration (called ''hopping'') between different nanocrystals. On the other hand, due to the higher band-gap energy of the surrounding nanocrystals or the thickness of the oxide several Si nanocrystals act as so-called ''traps'' for the excitons.[24,26] For lower temperatures, Eq. (4) is dominated by the $\exp(-\Delta E_{ij}/k_B T)$ term and for higher by the $\exp(-\gamma\cdot r_{ij})$ term. In other words, at high temperatures a migration of the excitons is more probable and at lower temperatures more Si nanocrystals act as an exciton trap. This mechanism of exciton ''hopping'' combined with a Gaussian size distribution explains the stretched exponential time decay of the PL signal.[24,25,28]

$$I(t) = I_0\exp\left[-\left(\frac{t}{\tau}\right)^b\right], \qquad (5)$$

where $I(t)$ is the PL intensity at the time t and b is the dispersion factor. The dispersion factor can be taken as a measure of the migration process. Totally isolated nanocrystals would show a single exponential time decay of their PL signal, i.e., a b value of unity. This mechanism was developed for porous Si and is only partially applicable to Si nanocrystals within a SiO_2 matrix. Nevertheless, the main features and trends should be comparable.[28]

III. EXPERIMENT

The nc-Si samples were prepared by alternative evaporation of SiO powder in either vacuum or oxygen atmosphere to create a SiO/SiO_2 superlattice. The synthesis procedure and the evaporation conditions are described elsewhere.[17,29] The thickness of the SiO layers varied between 1 and 6 nm. The SiO_2 layers had a thickness of 4 nm. The number of the superlattice periods was 45. The evaporated samples were annealed at 1100 °C in N_2 atmosphere. Photoluminescence measurements were performed using an Acton Research 500L spectrometer with an attached liquid nitrogen (LN) cooled charge coupled device (CCD) camera and a HeCd laser at 325 nm as the excitation source. The time resolved PL measurements were performed using a fast photomultiplier tube for detection and a pulsed nitrogen laser as the excitation source. Resonant PL measurements were done at liquid He temperature using a Ti-sapphire laser as the excitation source with an variable excitation wavelength between 800 and 1000 nm and a LN cooled CCD camera for detection. A D5005 (Siemens/Bruker AXS) x-ray diffractometer with a Cu $K\alpha$ source in the thin film diffraction mode was used for the x-ray diffraction (XRD) investigations.

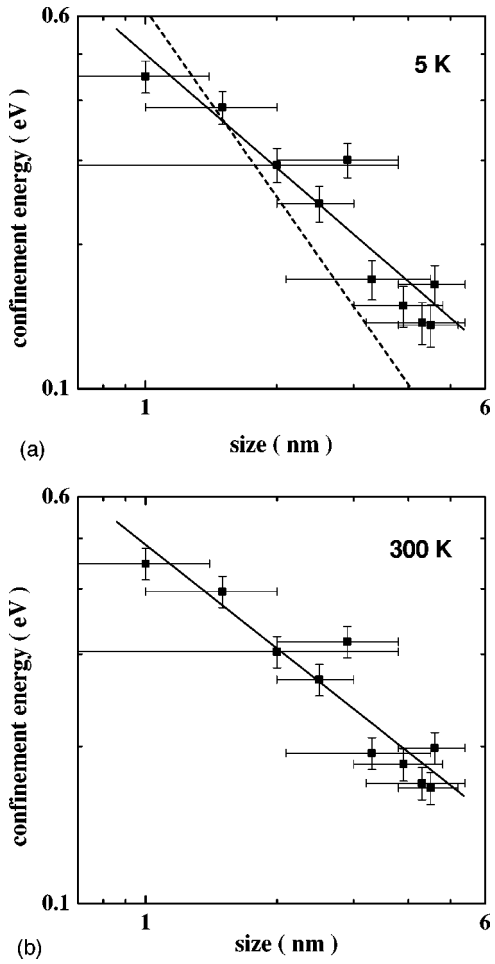

FIG. 1. Dependence of confinement energy on Si crystal size measured by XRD for PL measured at 4.5 K (a) and 300 K (b). The solid line shows a fit assuming a $D^{-0.8\pm0.1}$ (a) and a $D^{-0.6\pm0.1}$ (b) dependence of E_C. The dashed line in (a) shows a $D^{-1.3}$ dependence as described before (Refs. 11 and 21).

IV. RESULTS AND DISCUSSION

A. PL peak position

In Fig. 1 the nc-Si diameter (D) dependence of the confinement energy (E_C) is shown. The crystal size was measured by XRD using the Scherrer equation. E_C corresponds to the blueshift of the nc-Si PL band maximum measured at 4.5 K (a) and at 300 K (b) with respect to the band-gap energy of bulk silicon at these temperatures which reflects the net blueshift of the band gap as a combination of increasing band gap and increasing binding energy of the confined excitons, as introduced in Sec. II. The straight line in Fig. 1 represents the D^{-X} dependence of E_C with $X=0.8\pm0.1$ at 4.5 K (a) and $X=0.6\pm0.1$ at 300 K (b). The large error bars for the crystal size measured by XRD occur due to the limits of the measurement system arising from the very small crystal size and the overall layer thickness of about 200 nm. The PL energy shift shows the expected trends, but already the small difference between the results of the measurements at different temperatures indicates that the described blueshift of luminescence band with decreasing crystal size is not only determined by the confinement effect but also by another temperature dependent process.

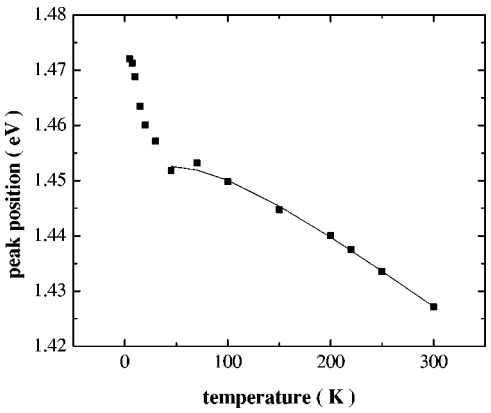

FIG. 2. PL peak position as a function of temperature for the sample with a 4-nm-thick SiO layer. The solid line shows the best fit to the experimental data from 50 to 300 K according to Eq. (6).

Figure 2(a) shows the peak position of the PL signal versus temperature for the sample with 4-nm-thick SiO layers after crystallization. The PL peak energy increases with decreasing temperature from 300 to 50 K similar to the temperature variation of the bulk silicon band gap and can be fitted by a relation given in (straight line):[30]

$$E_{\mathrm{gap}}(T)=E_{\mathrm{gap},0}-A\cdot\left(\frac{2}{\exp[\hbar\Omega/k_BT]-1}+1\right), \qquad (6)$$

where A is a temperature independent value (0.064 eV for bulk Si) and $\hbar\Omega$ stands for the average phonon energy (32 meV for bulk Si). $E_{\mathrm{gap},0}$ is the energy value determined by extrapolating the Si band gap from the linear part of its temperature dependence (from 300 to 100 K) to 0 K (1.233 eV for bulk Si). The best fit for our system can be achieved using $A=0.019\pm0.005$ eV, $E_{\mathrm{gap},0}=1.471\pm0.004$ eV where $E_{\mathrm{gap}}(T)$ is the mean nanocrystal band gap (energy position of the PL maximum), and $\hbar\Omega=24\pm4$ meV. This corresponds to a three times smaller A value compared to bulk Si and a smaller average phonon energy. However, for temperatures between 50 and 4.5 K, the experimental data does not follow the simple relation described by Eq. (6). The energy position of the PL peak increases rapidly with decreasing temperature from 1.45 to 1.472 eV. Figure 3 shows the full width at half maximum (FWHM) of the PL signal over the entire temperature range. Between 300 and 100 K the FWHM decreases with decreasing temperature from 257 to 245 meV. Surprisingly, for temperatures below 100 K the FWHM increases with decreasing temperatures up to 265 meV, which is even larger than the measured room temperature value.

To our opinion, these observations reflect the temperature dependence of the migration process [see Eqs. (3) and (4)]. For temperatures between 50 and 300 K the PL peak position follows Eq. (6). The change from an excitonic migration between all Si nanocrystals to a preferential migration from small to big nanocrystals can be seen by the decreasing FWHM of nearly exactly $k_B\Delta T$ with decreasing temperature and the three times smaller A value for the nc-Si compared to

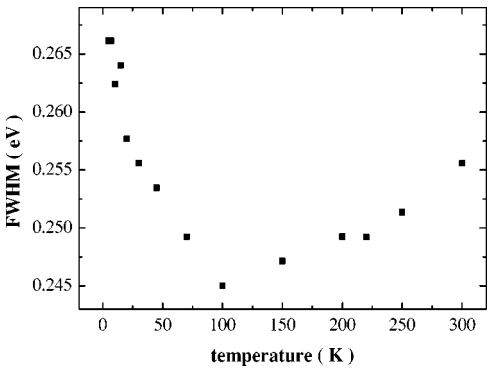

FIG. 3. FWHM of the PL signal as a function of temperature for the sample with a 4-nm-thick SiO layer.

bulk Si for the fit after Eq. (6). This smaller A value arises from the interplay between the band-gap behavior of Si and the changing size distribution which contribute to the PL signal. Below 50 K, the influence of the traps become more and more important. The effect of the thermalization of the excitons becomes smaller and smaller and more smaller crystals contribute to the PL signal. The FWHM increases again with decreasing temperature and the PL peak energy increase with decreasing temperature is more pronounced. These different size distributions of the Si nanocrystals which contribute to the PL signal at different temperatures can also explain the difference in the size dependence of E_C at 5 and 300 K.

B. Resonant excited PL measurements

Resonant excited PL was carried out in order to prove spatially confined excitons to be the origin of the PL signal. Figure 4 shows a set of resonantly excited PL spectra of a sample with a mean crystal size of 2.5 nm (initial SiO layer thickness of 4 nm). The different excitation energies (E_{ex}) are indicated by the position of the arrows. With decreasing excitation energy a steplike structure in the PL spectra becomes more pronounced. The energetical distance of the structures to E_{ex} agrees well with the energies of momentum conserving TO (56 meV) or TA phonons (19 meV) in Si for a recombination of electrons from the $\Delta_{1,C}$ point with holes

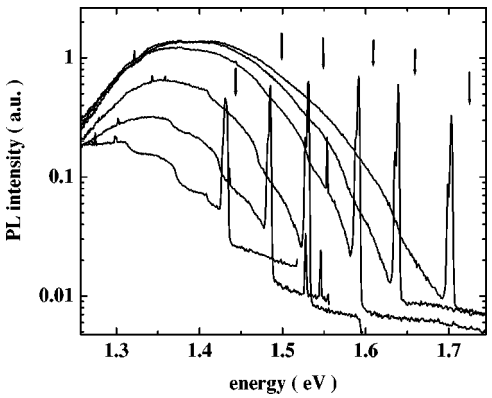

FIG. 4. Resonantly excited PL signal for different excitation energies (indicated by arrows) for the samples with a 4 nm SiO layer thickness after crystallization.

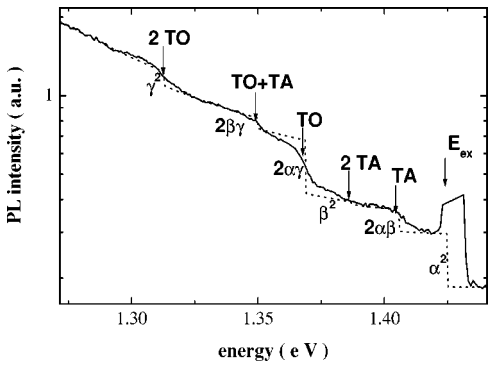

FIG. 5. Resonantly excited PL signal divided by the PL signal excited by low power UV light (straight line) and fitting function (dotted line) as described in the text.

from the $\Gamma_{25'}$ point. The resonant PL signal is determined by the Si nanocrystal size distribution and the absorption cross section of the Si nanocrystals which strongly depends on the difference between excitation and emission energy. To eliminate the effect of the size distribution, the resonantly excited PL signal was divided by the PL signal excited at low laser power in the UV ($\lambda_{ex}=325$ nm) which reflects the size distribution of the nanocrystals due to the very big differences between excitation and emission energies. The resulting steplike function is shown in Fig. 5. Every step height in this spectrum is a measure of the number of different no-phonon or momentum-conserving phonon-assisted absorption and recombination processes depending on their energy.[18] For the fit in Fig. 5 a set of three independent parameters α, β, and γ were introduced, which stand for the transition probabilities of the no-phonon (NP), TA phonon assisted, and TO phonon assisted process, respectively. The height of each step in the spectra is then fitted by the product of the absorption and emission probability and the sum of the possible processes. For the height of the first step only a NP absorption and emission can contribute to the PL signal (step height α^2). For the next step at an energy $E_{ex}-E_{TA}$ either a NP absorption and a TA phonon-assisted emission or a TA phonon-assisted absorption and a NP emission can contribute to the PL signal (step height $\alpha\beta+\beta\alpha$), and so on. Please note that due to the low measurement temperature of 4.5 K only phonon emission has to be taken into account. The increasing absorption cross section with increasing difference of excitation and emission energy was fitted by an exponential background. Additionally to the described phonon energies an offset had to be added to the excitation energy in order to place the steps at the right energy position. This offset corresponds to the quantum-confined-enhanced splitting energy ΔE_X,[10,11] as introduced in Eq. (1), and is between 3 and 5 meV. Its origin is the singlet-triplet splitting of the energy of the confined phonon due to the spin $\frac{1}{2}$ of electron and hole. The absorption into the singlet state is much more probable compared to the quasi-forbidden transition into the triplet state, while the recombination process at low temperatures (4.5 K) is dominated by the triplet state due to the thermal equilibrium. This difference in absorption and emission branch results in the described offset.

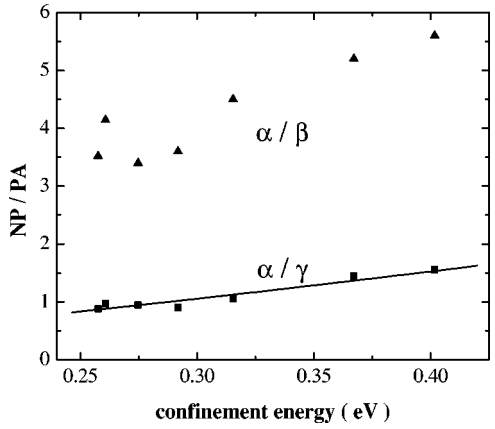

FIG. 6. Ratio of NP to TO phonon-assisted processes (triangles) and TA phonon-assisted processes (squares) as a function of E_C. The solid line is a theoretical fit assuming a $E_C^{1.7}$ dependence of the increasing ratio of NP to TO phonon-assisted processes.

In Fig. 6 the ratio of NP to phonon assisted processes, determined by the fitting procedure described above, is plotted over E_C. E_C is determined by the difference between the Si band gap at 4.5 K and the excitation energy for the resonant excitation. As can be seen here, a significant increase of the relative NP transition probability with increasing E_C is observed. The ratio of NP process probability to the probability of the TO phonon assisted process was fitted and scales with $E_C^{1.7}$ represented by a solid line in Fig. 6. Taking into account that E_C scales as $D^{-0.8\pm0.1}$ [see Fig. 1(a)] and that the phonon-assisted recombination probability scales with the volume of the nc-Si,[18] which means with D^{-3}, one can calculate that the NP recombination probability scales with $D^{-4.5}$. Theoretically, a D^{-6} dependence of NP transition probability was calculated[31] and experimentally proven for porous Si.[18] In both cases the vacuum level as the barrier for the exciton confined within the nc-Si can be assumed to be infinite. The absolute value of the NP process probability to the probability of the TO phonon assisted processes ratio is above 1 for E_C higher than 0.3 eV, which is a rather high ratio compared to similar systems.[18] The smaller dependence and the enhanced absolute value of NP transition for the same E_C values could be explained by the finite potential barrier due to the SiO_2 matrix. A lower SiO_2 barrier leads to a smearing out of the electron wave function into the suboxide. In this case, a NP transition strength enhancement is more likely due to the amorphous structure of the SiO_2. Furthermore, this effect to our opinion is also responsible for a smaller sensitivity of the PL energy to nanocrystal size in our layers compared to porous silicon: a lower potential barrier implies a smaller confinement energy for excitons. This would explain the still very low exponent of 0.8 for the size dependence of E_C (see Fig. 1) at a temperature of 5 K where migration effects are negligible.

C. Temperature dependence of the PL lifetime

Figure 7(a) shows the temperature dependence of PL lifetime and PL intensity for temperatures between 300 and 4.5 K for the sample with a nc-Si mean size of 2.5 nm. The PL

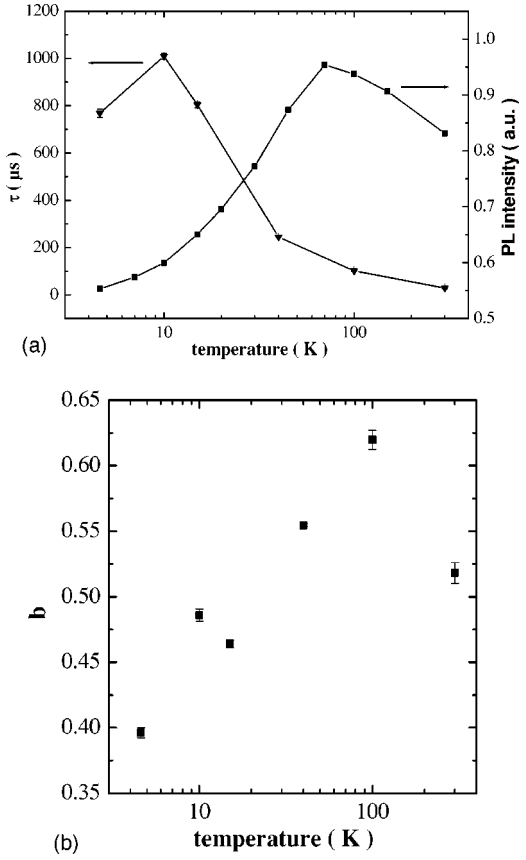

FIG. 7. Temperature dependence of PL intensity, (a) lifetime and (b) of the *b* value introduced in Eq. (5) for the sample with an initially 4-nm-thick SiO layer.

intensity increases with decreasing temperature between 300 and 70 K and decreases again for temperatures lower than 70 K. The lifetime of the observed luminescence increases for decreasing temperature over the whole measured range from 28 μs at 300 K to 770 μs at 4.5 K. The lifetimes were obtained by fitting the experimental data by a stretched exponential fit according to Eq. (5).

The *b* values for the different temperatures are shown in Fig. 7(b). For temperatures below 100 K, *b* is decreasing with decreasing temperature. For a temperature of 300 K a smaller *b* value compared to the 100 K value was found. The *b* value is between 0.4 and 0.62 over the whole temperature range. *b* is emission energy independent at temperatures of 300 and 4.5 K and decreases with increasing emission energy for a measurement temperature of 100 K (not shown here). This temperature dependence of the *b* values proves the occurrence of a migration of excitons between the Si nanocrystals. Decreasing *b* with decreasing temperature indicates an increasing influence of traps on the exciton migration and was observed and simulated by Monte Carlo simulation before.[24,26,28] At 300 K the additional influence of a nonradiative recombination channel results in a decreased *b* value compared to measurements at 100 K. The energy dependence of *b* does also fit to the described mechanism. At high temperatures (300 K) the exciton migration is nanocrystal size independent and so is the *b* value. At lower temperatures (100 K), the exciton migration does preferentially take place

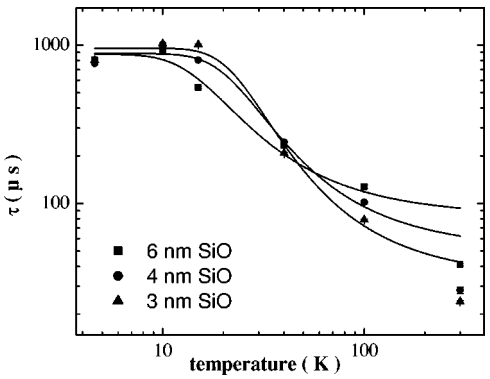

FIG. 8. Temperature dependence of PL lifetime of the samples with 6-, 4-, and 3-nm-thick SiO layers, detection wavelengths are 850, 800, and 750 nm, respectively. The straight lines are fits according to Eq. (1) for the experimental values from 4.5 to 100 K.

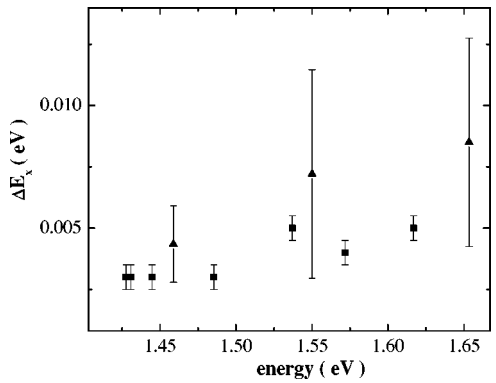

FIG. 9. Energy dependence of E_X determined from offset in the resonantly excited PL (squares) and from the temperature dependent PL lifetime (triangles).

from smaller to bigger crystals (thermalization) and the b value decreases for increasing emission energy, i.e., decreasing crystal size. At even lower temperatures (4.5 K) the exciton migration is dominated by traps and the b value becomes again emission energy independent.

The temperature dependence of the lifetime for different emission energies measured on the sample with 3-, 4-, and 6-nm-thick SiO layers is shown in Fig. 8. The straight lines stand for fits which correspond to Eq. (1) assuming a singlet-triplet splitting of the excitonic state due to electron–hole exchange interaction. The experimental data for the PL lifetime at 300 K differs significantly from the fit due to the fact that the measured lifetime of the nc-Si PL signal is a combination of radiative and nonradiative recombination channels as well as migration effects of the excitons.[24,25,28] Nonradiative recombination channels and migration effects play a major role at these temperatures. This agrees well with a smaller PL intensity {see Fig. 7(a) and the smaller b value at 300 K [see Fig. 7(a)]} in comparison to the measurements at 100 K. The results for the described fits are summarized in Table I. The decreasing singlet lifetime with increasing detection energy and the values of singlet and triplet lifetimes as well as the value of the splitting energy ΔE_X are in agreement with the quantum confinement model.

In Fig. 9, the values for ΔE_X are shown depending on the emission energy measured by the temperature dependence of the lifetime and the offset in the resonantly excited PL. ΔE_X increases with increasing emission energy for both fitting procedures. The values of ΔE_X measured spectroscopically with resonant PL excitation are found to be a bit smaller than those extracted from the temperature dependence of the lifetime. The possible variation of nanocrystal shapes and sizes results in the absence of the unique value of ΔE_X even at the same energy of confinement. The optically measured ΔE_X is the minimal value in the distribution of all possible ΔE_X, whereas the splitting deduced from temperature dependence can be considered rather as an average one.[10]

TABLE I. Fitting parameter for the fits in Fig. 8 concerning Eq. (1).

SiO thickness (nm)	E_{det} (eV)	τ_{sing} (μs)	τ_{trip} (μs)	ΔE_X (meV)
6	1.46	20 ± 10	900 ± 100	4 ± 1
4	1.55	13 ± 10	850 ± 90	7 ± 4
6	1.65	9 ± 5	960 ± 70	9 ± 4

V. CONCLUSIONS AND SUMMARY

Experimental data on the temperature behavior of the PL from the nc-Si presented here can only be explained assuming excitation migration between Si nanocrystals. The increasing emission energy with decreasing nc-Si size, the observed Si momentum-conserving phonon-related structure in the resonantly excited PL signal, the temperature behavior of the PL lifetime arising from exciton exchange splitting, and the decreasing singlet lifetime with increasing emission energy clearly indicate that the PL originates from exciton recombination within the nc-Si.

The discussed quantum confinement effects show qualitatively the same trends as described for other systems[18,21] but differ quantitatively from these systems due to the difference in size distribution and surrounding matrix. A possible explanation for the quantitative differences for several confinement effects is exciton migration between different Si nanocrystals. The migration process involves a thermalization of the excitons, which means that the excitons migrate into the energetically most favorable low energy state. This can be seen from the temperature dependence of the PL lifetime as described in Sec. IV C. The temperature dependence of the PL peak position (see Fig. 2) and its FWHM (see Fig. 3) further reflect the described temperature dependence of the exciton migration process efficiency. This indicates a significant influence of the excitonic migration on the optical properties of our layers. The very low b values measured for the time dependence of the PL lifetime of the size-controlled nc-Si system in comparison with porous Si and nc-Si in SiO_2 produced by ion implantation[28] indicates a very effective migration process. The very high density of Si nanocrystals of nearly the same size result in small r_{ij} and ΔE_{ij} values in Eqs. (3) and (4) which lead to a high exciton migration probability.

On the other hand, the migration effect can only partially explain the differences of the optical properties of the described system compared to porous Si (Ref. 11) or theoretical calculations.[19,22] Especially, the measurements at low temperatures, where the thermalization of the excitons due to migration effects can be neglected, indicate the existence of a layer with a lower confinement barrier compared to thermally grown SiO_2 around the Si nanocrystal. The process of the phase separation of the SiO_x into Si and SiO_2 makes the existence of a SiO_x shell around the Si nanocrystals probable. A lower band gap of the surrounding matrix leads also to a higher absolute value of NP transition probability and to a higher migration probability, which could explain the very strong migration effects mentioned above.

In conclusion, the observed effects can be clearly assigned to quantum confined electron–hole recombination within the nc-Si. Increasing confinement energy and NP transition probability with decreasing crystal size were shown. The size dependence of all the described properties indicates a lower effective barrier height of the SiO_2 matrix compared to similar systems. The smaller band gap of surrounding matrix and very high density of nearly monodispersed Si nanocrystals lead to a very high migration probability of the excitons between the crystals. This can explain the quantitative size dependence of the different confinement effects.

ACKNOWLEDGMENT

This work was financially supported by the German Research Foundation (ZA191/14-2).

*Present address: Memory Development Center, Infineon Technologies Corporation, Königsbrücker Strasse 180, D-01099 Dresden, Germany.

†Corresponding author. Electronic address: zacharia@mpi-halle.de

[1] L. T. Canham, Appl. Phys. Lett. **57**, 1046 (1990).
[2] V. Lehmann and U. Gösele, Appl. Phys. Lett. **58**, 856 (1991).
[3] G. Ghislotti, B. Nielsen, P. Asoka-Kumar, K. G. Lynn, A. Gambhir, L. F. Di Mauro, and C. E. Bottani, J. Appl. Phys. **79**, 8660 (1996).
[4] Y. Kanemitsu, Phys. Rev. B **49**, 16845 (1994).
[5] T. Shimizu-Iwayama, D. E. Hole, and P. D. Townsend, Nucl. Instrum. Methods Phys. Res. B **148**, 980 (1999).
[6] M. L. Brongersma, A. Polman, K. S. Min, E. Boer, T. Tambo, and H. A. Atwater, Appl. Phys. Lett. **72**, 2577 (1998).
[7] T. Shimizu-Iwayama, D. E. Hole, and I. W. Boyd, J. Phys.: Condens. Matter **11**, 6595 (1999).
[8] M. Zhu, Y. Han, R. B. Wehrspohn, C. Godet, R. Etemadi, and D. Ballutaud, J. Appl. Phys. **83**, 5386 (1998).
[9] X. Wu, A. M. Bittner, K. Kern, C. Eggs, and S. Veprek, Appl. Phys. Lett. **77**, 645 (2000).
[10] P. D. J. Calcott, K. J. Nash, L. T. Canham, M. J. Kane, and D. Brumhead, J. Phys.: Condens. Matter **5**, L91 (1993).
[11] D. Kovalev, H. Heckler, G. Polisski, and F. Koch, Phys. Status Solidi B **215**, 871 (1999).
[12] S. Hayashi, Y. Kanzawa, T. Kageyama, S. Takeoka, M. Fujii, and K. Yamamoto, Solid State Commun. **102**, 533 (1997).
[13] U. Kahler and H. Hofmeister, Opt. Mater. (Amsterdam, Neth.) **17**, 83 (2001).
[14] F. Huisken, B. Kohn, and V. Paillard, Appl. Phys. Lett. **74**, 3776 (1999).
[15] J. St. John, J. L. Coffer, Y. Chen, and R. F. Pinizzotto, J. Am. Chem. Soc. **121**, 1888 (1999).
[16] Y. Hirano, F. Sato, N. Saito, M. Abe, S. Miyazaki, and M. Hirose, J. Non-Cryst. Solids **266-269**, 1004 (2000).
[17] M. Zacharias, J. Heitmann, R. Scholz, U. Kahler, M. Schmidt, and J. Bläsing, Appl. Phys. Lett. **80**, 661 (2002).
[18] D. Kovalev, H. Heckler, M. Ben-Chorin, G. Polisski, M. Schwartzkopf, and F. Koch, Phys. Rev. Lett. **81**, 2803 (1998).
[19] C. Delerue, G. Allan, and M. Lannoo, Phys. Rev. B **48**, 11024 (1993).
[20] Y. Kayanuma, Phys. Rev. B **38**, 9797 (1988).
[21] G. Ledoux, O. Guillois, D. Porterat, C. Reynaud, F. Huisken, B. Kohn, and V. Paillard, Phys. Rev. B **62**, 15942 (2000).
[22] J. P. Proot, C. Delerue, and G. Allan, Appl. Phys. Lett. **61**, 1948 (1992).
[23] V. A. Burdov, Semiconductors **36**, 1154 (2002).
[24] H. E. Roman and L. Pavesi, Condens. Matter **8**, 5161 (1996).
[25] L. Pavesi, J. Appl. Phys. **80**, 216 (1996).
[26] L. Pavesi and M. Ceschini, Phys. Rev. B **48**, 17625 (1993).
[27] E. Martin, C. Delerue, G. Allan, and M. Lannoo, Phys. Rev. B **50**, 18258 (1994).
[28] J. Linnros, N. Lalic, A. Galeckas, and V. Grivickas, J. Appl. Phys. **86**, 6128 (1999).
[29] M. Zacharias, L. X. Yi, J. Heitmann, R. Scholz, M. Reiche, and U. Gösele, Solid State Phenom. **94**, 95 (2003).
[30] P. Y. Yu and M. Cardona, *Fundamentals of Semiconductors* (Springer-Verlag, Berlin, 1996).
[31] M. S. Hybertsen, Phys. Rev. Lett. **72**, 1514 (1994).